

Electronic Supplementary Information (ESI)

Environmental and economic assessment of glycerol oxidation to dihydroxyacetone over technical iron zeolite catalysts

Giacomo M. Lari,^a Cecilia Mondelli,^a Stavros Papadokonstantakis,^{*b} Merten Morales,^a
Konrad Hungerbühler^a and Javier Pérez-Ramírez^{*a}

^a*Institute for Chemical and Bioengineering, Department of Chemistry and Applied Biosciences, ETH Zurich, Vladimir-Prelog-Weg 1, CH-8093 Zurich, Switzerland. Fax: +41 44 6331405 Tel: +41 44 6337120; E-mail: jpr@chem.ethz.ch*

^b*Division of Industrial Energy Systems and Technologies, Department of Energy and Environment, Chalmers University of Technology, Kemivägen 4, SE-41296, Gothenburg, Sweden, Tel: +46 31 7728533; E-mail: stavros.papadokonstantakis@chalmers.se*

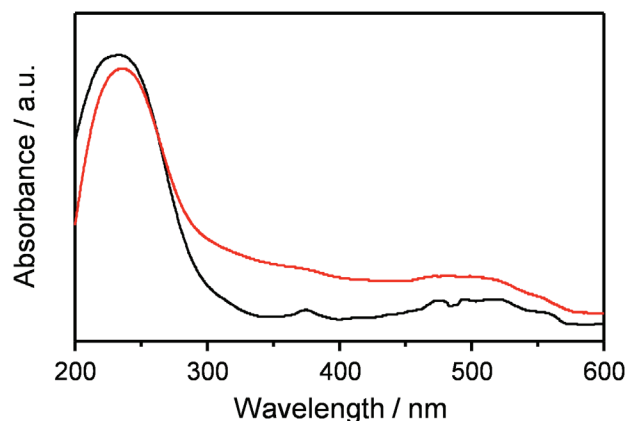


Fig. S1. UV-Vis spectra of the FeS-si-P-cs before (black) and after (red) reaction.

1. Isomerisation of dihydroxyacetone to methyl lactate over tin-containing MFI zeolites

1.1. Catalyst synthesis

A tin-containing MFI zeolite was prepared by hydrothermal synthesis following a reported procedure.¹ Briefly, tetraethyl orthosilicate (TEOS, 93.5 g, Sigma-Aldrich, 98%) was mixed with a solution of $\text{SnCl}_4 \cdot 5\text{H}_2\text{O}$ (1.27 g, Sigma-Aldrich, 98%) in deionised H_2O (29.9 g) and allowed to react for 30 min under stirring. Then, tetrapropylammonium hydroxide (TPAOH, 198 g, Alfa Aesar, 20 wt.%) was added dropwise and the mixture was stirred for 1 h. Finally, 84 g of deionised H_2O were added and the solution was stirred for 30 min. The obtained sol (0.008 SnO_2 : 1 SiO_2 : 0.44 TPAOH : 31.5 H_2O on mole basis) was transferred into a 500- cm^3 Teflon-lined autoclave and heated at 433 K for 3 days under static

conditions. Thereafter, the zeolite crystals were separated by filtration, washed thoroughly with deionised water, dried overnight at 338 K and calcined in static air at 823 K (5 K min^{-1}) for 5 h to ensure the complete removal of the organic structure directing agent. Subsequently, they were converted into the protonic form by three consecutive ion exchanges in a 0.1 M aqueous NH_4NO_3 solution (6 h, 298 K, 100 cm^3 per gram of dried zeolite) followed by calcination under the conditions mentioned above.

1.2. Catalyst testing

The conversion of dihydroxyacetone (DHA) into methyl lactate (ML) was studied using a homemade continuous-flow reactor setup comprising (i) an HPLC pump (Gilson-306), (ii) a stainless steel tubular reactor with a pre-column (Swagelok SS-T4-S-035, i.d. = 4.6 mm), both heated in a tubular oven and (iii) a backpressure regulator (Swagelok, LH2981001). The reactor was loaded with a mixture of the catalyst (0.25 g) diluted with quartz (0.3 g, particle size = 0.25-0.36 mm) and heated at 383 K. Thereafter, a liquid feed ($0.4 \text{ cm}^3 \text{ min}^{-1}$) was admitted which contained 0.50 M DHA, 1 M H_2O , 0.01 M pyruvaldehyde, 5 mM pyruvic acid and 4 mM acetic acid in methanol, and thus corresponded to the condensate obtained from the chemocatalytic oxidation of glycerol after a 15-fold dilution with methanol. To prevent evaporation at the reaction temperature, the system was pressurised to 25 bar prior to heating. Samples were periodically collected at the outlet of the reactor, diluted by addition of known amounts of water and analysed by high-performance liquid chromatography (HPLC) using the same instrument and method as described for the analysis of the glycerol oxidation condensate in the main manuscript. The amount of ML produced was determined using a gas chromatograph (HP 6890) equipped with an HP-5 capillary column and a flame ionisation detector. Quantification was accomplished by integration of its peak using isooctane (Fluka, 99.5%) as an internal standard. Conversion and selectivity data were calculated as detailed in the main manuscript.

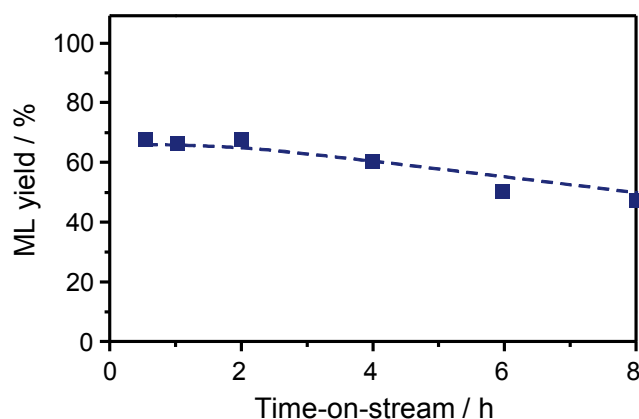


Fig. S2. ML yield as a function of time on stream.

2. Process modelling

2.1. Production of DHA from crude GLY for lactic acid production

Here, we refer to the part of the flowsheet (see Fig. 2 in the main manuscript) for converting crude GLY to DHA that can be further utilised to produce lactic acid (LA). The process can be roughly divided into three steps: (i) upstream processing of crude GLY for removing ash, MONG and methanol, (ii) chemocatalytic gas-phase oxidation of GLY to DHA and by-products and (iii) condensation of the reactor effluent to remove gases and obtain a concentrated solution of DHA in water while recovering heat for process integration. These steps are described in detail below with respect to process conditions and modelling assumptions.

Step-1: Upstream processing of crude GLY for removing ash, MONG and methanol

The crude GLY composition and upstream processing correspond to those reported by Morales *et al.*² The same modelling assumptions are used for the sake of comparison. The ash in the crude GLY is almost completely separated (99%) by conventional filtration (SSPLIT filter in Aspen Plus[®] V8.6) and used for landfill according to the Ecoinvent model (Version 3, Landfill, ash from paper).³ Since in 70% of the US biodiesel production, sodium methylate represents the main constituent of the ash fraction, it is assumed that the ash solely comprises this chemical species.² The crude GLY stream is then treated through flash evaporation (FLASH2 separator in Aspen Plus[®] V8.6) at ambient pressure and 463 K to remove most of the methanol (92%) and the water (85%). The subsequent separation of MONG is not rigorously modelled. Although the technology for MONG separation from crude GLY is industrialised by PALL[®],⁴ a SEP separator in Aspen Plus[®] V8.6 is simply applied assuming 100% separation of MONG and of the remaining ash due to the lack of data on the process and as done in the work by Morales *et al.*² Two scenarios are considered for the fate of the methanol and MONG waste streams, *i.e.*, both streams are treated in conventional waste water treatment or in a waste-to-energy incineration facility, modelled according to Rerat *et al.*⁵ The upstream processing of crude GLY produces an inlet stream for the reactor consisting of 98.5 wt.% GLY, 1.2 wt.% water and 0.3 wt.% methanol.

Step-2: Chemocatalytic gas-phase oxidation of GLY to DHA and by-products

The GLY-containing stream from step-1 is evaporated at ambient pressure and 559 K, heated up to the reaction temperature (623 K) and mixed with compressed, hot air (2 bar, 623 K) at the inlet of the reactor. The air:GLY mass ratio is 8, corresponding to a molar O₂:GLY ratio of 5.3. For the process assessment of this unit, the use of yield-related information of the reactions taking place in the chemocatalytic gas-phase oxidation of GLY to DHA is sufficient, which are summarised in Table S1. Detailed information about the reaction kinetics, mass and heat transfer phenomena, pressure drop, *etc.*, would be required for a detailed design of a full-scale, plug-flow reactor, which is outside the scope of the present study. It should be noted that the yields presented in Table S1 do not coincide with those derivable from Table 4 of the main manuscript, since these data refer to 72 h and between 1 and 2 h on stream, respectively. The process is modelled with an isothermal RSTOIC reactor in Aspen Plus[®] V8.6. The reactor is also loaded with 153 g of the FeS-si-P-cs catalyst for 100 h operation and a production rate of 1 kg_{DHA} h⁻¹. After 100 h on stream, the catalyst is replaced and disposed (according to zeolites data from Ecoinvent, Version 3).³

Table S1 Reactions and yields considered in the process model of the gas-phase oxidation of GLY over the FeS-si-P-cs catalyst. The products are abbreviated as in Table 4 of the main manuscript (*i.e.*, PAI: pyruvaldehyde, PAc: pyruvic acid, Other: acetol, acetaldehyde, acetic acid, acrolein and acrylic acid)

Reaction	Yield (%)	Product
$C_3H_8O_3 + 0.5O_2 \rightarrow C_3H_6O_3 + H_2O$	76.2	DHA
$C_3H_8O_3 + 0.5O_2 \rightarrow C_3H_4O_2 + 2H_2O$	0.8	PAI
$C_3H_8O_3 + O_2 \rightarrow C_3H_4O_3 + 2H_2O$	1.5	PAc
$C_3H_8O_3 + 1.5O_2 \rightarrow C_2H_4O_2 + 2H_2O$	0.5	Other
$C_3H_8O_3 + 3.5O_2 \rightarrow 3CO_2 + 4H_2O$	21.2	CO ₂

Step-3: Condensation of the reactor effluent to remove gases

The reactor effluent contains 84.3 wt.% air-related gases (*i.e.*, unreacted O₂ and inert N₂ and Ar), 8.3 wt.% DHA, 3.7 wt.% H₂O, 0.3 wt.% of organic by-products and methanol and 3.4 wt.% CO₂. This hot gas stream must be cooled down to nearly ambient conditions (*e.g.*, 303 K, assuming cooling water available at 283 K and a 20 K minimum temperature approach in the heat exchangers) to condense and separate DHA from the gases. This results in a liquid stream with the following composition: 76.5 wt.% DHA, 22.0 wt.% water, 1.3 wt.% of organic by-products and methanol and 0.2 wt.% of dissolved gases.

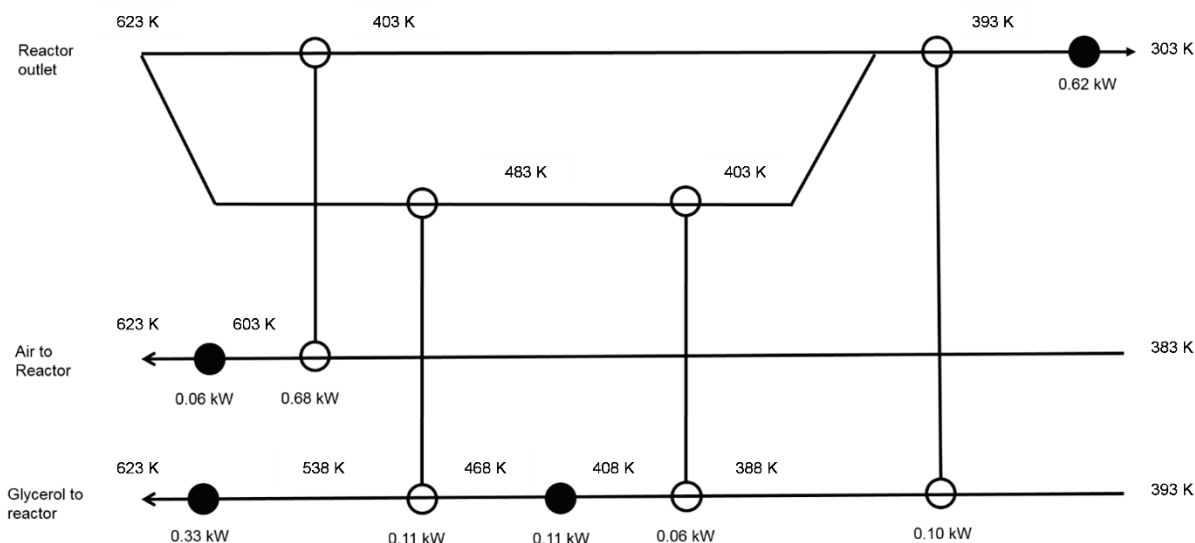


Fig. S3 Heat exchanger network for the recovery of the heat content of the gas stream at the outlet of the reactor and with a minimum temperature approach of 20 K. The white circles denote heat exchange between process streams and the black circles externally provided heating and cooling.

According to the evidences herein gathered (Fig. S1), this stream is suitable to be sent to a chemocatalytic lactic acid production process in methanol using a Sn-MFI catalyst, which has been described by Morales *et al.*² Upon the condensation, only 0.1% of DHA is lost in the gas stream, which is assumed to be sent to

the flare stack of the industrial site. It should be noted that this gas stream is the main source of the process direct CO₂ emissions, as it also contains the CO₂ produced by the full oxidation reaction in Table S1.

It should also be noted that the gas stream at the outlet of the reactor is the main source for heat integration in this process. Fig. S3 presents the heat exchanger network (HEN) for the recovery of this heat content. Without heat integration, the process requires external heating for 1.44 kW kg_{DHA}⁻¹ and external cooling for 1.56 kW kg_{DHA}⁻¹. With heat integration, the required external energy is reduced to 0.50 kW kg_{DHA}⁻¹ of heating and 0.62 kW kg_{DHA}⁻¹ of cooling. The theoretical targets for external energy requirements, calculated by approximate pinch-analysis (*i.e.*, assuming linear functions of heating requirements with temperature for sensible and latent heat of pure components and mixtures, not presented here in detail) and a conservative 20 K minimum temperature approach in the heat exchangers, are 0.24 kW kg_{DHA}⁻¹ of heating and 0.36 kW kg_{DHA}⁻¹ of cooling. Therefore, the heuristically designed HEN (Fig. S3) recovers approximately 65% of the heating requirements and 80% of the theoretical heat recovery targets.

2.2. Purification of dihydroxyacetone

Here we refer to the part of the flowsheet (Fig. 2 in the main manuscript) where the condensed DHA stream is further treated to produce pure DHA. The solubility of DHA in water is 930 g l⁻¹ at 293 K.⁶ This means that at the conditions of the liquid stream out of the condenser (*i.e.*, 303 K, 1 kg_{DHA}/0.29 kg_{H₂O}) one would have approximately 0.27 kg of DHA dissolved in water (*i.e.*, neglecting the effects on solubility due to the presence of the organic by-products and methanol), and only 0.73 kg of DHA precipitated as solid. Therefore, a cooling crystallisation out of water would not be an effective separation procedure. Taking into account the relatively small amounts of water, an evaporative crystallisation is considered in this study. The DHA crystallisation unit in Fig. 2 in the main manuscript represents an integrated evaporative crystallisation process consisting of five evaporation steps in series (*i.e.*, in an integrated five-effect evaporation set-up modelled using FLASH2 separators and a CRYSTALLIZER solid model in Aspen Plus[®] V8.6) at reducing pressures and temperatures (Table S2). The operating temperatures and pressures keep DHA in the liquid phase until the final vacuum effect (*i.e.*, the melting point of DHA is 369 K⁶). Due to the presence of small amounts of water, the respective residence times in large scale evaporators (*e.g.*, operating at 1 t h⁻¹) are going to be relatively small, reducing the risk for stability problems of DHA at higher temperatures. The overall loss of DHA in the gas streams of the evaporative crystallisation process is approximately 3%.

The gas stream of any evaporation effect is first cooled down to recover energy that can be used in the next effects (*i.e.*, operating at lower pressures and, therefore, temperatures). Then, it is further cooled down to 298 K and treated as wastewater. The DHA after the last vacuum effect is taken in solid form by cooling at 353 K, further washed (SWASH solid model in Aspen Plus[®] V8.6) with acetone and finally dried with air at 353 K (DRYER solid model in Aspen Plus[®] V8.6). The acetone : DHA mass ratio in the input and output of the washer is set to 2 and the air : liquid mass ratio in the dryer is set to 1. Acetone is assumed to be completely separated from air in a vacuum degasifier (SEP separator in Aspen Plus[®] V8.6) and recycled back to the washing process after purging 2% of the recycling stream to avoid accumulation mainly of water, acetic acid and pyruvic acid. Pyruvic acid and acetic acid are assumed to remain in the liquid phase because their melting points are 286 K and 290 K, respectively.^{7,8} This purge stream is sent to a waste incineration facility. The solid stream in the output of the drier is, therefore, assumed to be

100% pure DHA, while the loss of DHA in the washing procedure is 0.1% (*i.e.*, mainly due to the purge stream in the recycling of acetone).

A separate heat integration is applied for the purification part (*i.e.*, treating 1 kg_{DHA} h⁻¹), reducing the external heating from 0.95 kW to 0.63 kW and the external cooling from 0.85 kW to 0.53 kW. This part of the process does not present high integration potential because of the generally lower temperature gradients, even in the multi-effect evaporation. The 0.95 kW of thermal energy are divided into 0.30 kW for the five evaporation effects, 0.32 kW for the dryer and 0.33 kW for the acetone recovery. Out of these, 0.08 kW are recovered for the evaporation effects, 0.17 kW for the dryer and 0.07 kW for the acetone recovery. The heuristically designed HEN (Fig. S4) considers a realistic minimum temperature approach of 10 K.

Table S2. Operating conditions, DHA purity and recovery in the 5-effect evaporative crystallisation

Effect	Pressure (bar)	Temperature (K)	DHA (wt.%)	DHA recovery/effect (%)
1	3.5	433	80.0	99.8
2	1.6	413	85.7	99.7
3	0.4	398	95.2	99.0
4	0.1	383	98.3	99.4
5	Vacuum (10 mbar)	368	99.4	99.2

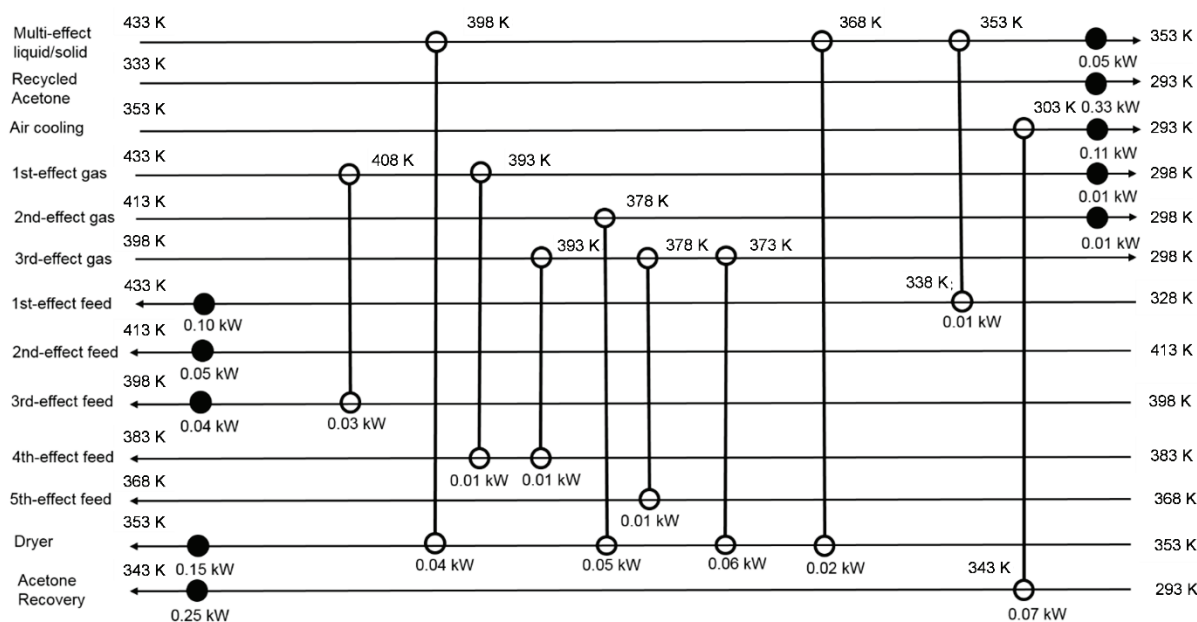


Fig. S4. Heat exchanger network for the purification of the DHA with a minimum temperature approach of 10 K. Only the most important heat exchanges are presented for sake of clarity (*i.e.*, heat exchanges lower than 0.01 kW are not depicted). The white circles denote heat exchange between process streams and the black circles externally provided heating and cooling.

3. Process assessment of alternative scenarios

Besides the main scenarios compared in the manuscript, additional scenarios were also generated with respect to the following factors:

- Setting a higher crude GLY price (270 USD t⁻¹, which was the pure GLY price reported by Morales *et al.*² compared to 111 USD t⁻¹ used in their manuscript (and also here) for crude GLY)
- Treating the methanol and MONG waste streams of the upstream crude GLY processing in waste-to-energy incineration plants
- Using more detailed models than Morales *et al.*² for the washing-drying process of DHA (*i.e.*, leading to higher losses of acetone)

These scenarios are coded with three binary indices (0,1) in the order presented above, added to the notation of Table 2 in the main manuscript. For example, CHEMO-1A-001 refers to the case in which the reference value of crude GLY is used (111 USD t⁻¹), the methanol and MONG waste streams are sent to wastewater treatment plants, but a more detailed model for the washing-drying process of DHA is applied. CHEMO-1B-00 denotes the same scenario as CHEMO-1B in the main manuscript (there is no third index, since this is a DHA for LA scenario, where no washing-drying of DHA takes place), while CHEMO-1B-10 denotes the scenario where a higher price of crude GLY is used, and so on. The process assessment results in terms of operating cost, CED, GWP and EI99 for these scenarios are presented in Table S3.

Table S3 Process assessment for additional scenarios including higher crude GLY price, alternative treatment of methanol- and MONG-containing waste streams and more detailed modelling of the washing-drying processes for the purification of DHA. The coding of these scenarios is explained in the text.

Scenario	Operating cost (USD kg _{DHA} ⁻¹)	CED (MJ _{eq} kg _{DHA} ⁻¹)	GWP-100a (kg _{CO2-eq} kg _{DHA} ⁻¹)	EI99 (points kg _{DHA} ⁻¹)
CHEMO-1A-000	0.41	51.4	1.03	0.16
CHEMO-1A-001	0.58	60.6	1.71	0.20
CHEMO-1A-010	0.41	37.5	0.64	0.12
CHEMO-1A-011	0.58	46.7	1.32	0.16
CHEMO-1A-100	0.71	51.4	1.03	0.16
CHEMO-1A-101	0.88	60.6	1.71	0.20
CHEMO-1A-110	0.71	37.5	0.64	0.12
CHEMO-1A-111	0.88	46.7	1.32	0.16
CHEMO-2A-000	0.41	-3.8	-0.31	0.01
CHEMO-2A-001	0.58	5.4	0.37	0.04
CHEMO-2A-010	0.41	-17.7	-0.70	-0.03
CHEMO-2A-011	0.58	-8.5	-0.02	0.00
CHEMO-2A-100	0.71	-3.8	-0.31	0.01
CHEMO-2A-101	0.88	5.4	0.37	0.04
CHEMO-2A-110	0.71	-17.7	-0.70	-0.03
CHEMO-2A-111	0.88	-8.5	-0.02	0.00
CHEMO-1B-00	0.32	44.7	0.65	0.14
CHEMO-1B-01	0.32	31.2	0.27	0.10
CHEMO-1B-10	0.61	44.7	0.65	0.14
CHEMO-1B-11	0.61	31.2	0.27	0.10
CHEMO-2B-00	0.32	-8.8	-0.65	-0.01
CHEMO-2B-01	0.32	-22.3	-1.03	-0.05
CHEMO-2B-10	0.61	-8.8	-0.65	-0.01
CHEMO-2B-11	0.61	-22.3	-1.03	-0.005

4. Background data for the environmental and economic assessment

The background data used in this study for the environmental and economic assessment with respect to the consumption of resources are presented in Table S4, while those related to the environmental impact of the process emissions (*i.e.*, those generated by the incineration units, waste water treatment plants and the direct CO₂ emissions) are presented in Table S5.

Table S4 Background data for the environmental (without renewable resources) and economic assessment with respect to resources consumption and waste treatment (sources: Ecoinvent database³, www.alibaba.com and ref. [9])

Substance	CED (MJ _{eq} kg ⁻¹)	EI99 (Points kg ⁻¹)	GWP (kg _{CO2-eq} kg ⁻¹)	Price (USD t ⁻¹)
Process water	2.8 10 ⁻⁴	1.8 10 ⁻⁶	2.4 10 ⁻⁵	1
Acetone	46.2	0.17	1.18	685
Zeolites	73.7	0.39	4.20	400
Crude GLY - INC	-19.7	-0.063	0.20	111
Crude GLY - WWTP	9.97	0.021	0.92	111
Heat*	1.57	0.01	0.10	20
Electricity*	9.87	0.02	0.49	0.10
Cooling water from river	0.00	0.00	0.00	0.15
Natural gas*	1.24	4.0 10 ⁻³	1.2 10 ⁻²	0.01
Catalyst (zeolite) disposal	0.16	7.6 10 ⁻⁴	5.0 10 ⁻³	---

*Heat is measured in MJ and electricity in kWh.

Table S5 Background data for the environmental impact of the emissions (source: Ecoinvent database³)

Substance	EI99 (Points kg ⁻¹)	GWP (kg _{CO2-eq} kg ⁻¹)
Carbon dioxide	0.0546	1
Nitrogen dioxide	2.75	1.57

5. References

- [1] N. K. Mal, V. Ramaswamy, P. R. Rajamohan and A. V. Ramaswamy, *Microporous Mater.*, 1997, **12**, 331.
- [2] M. Morales, P.Y. Dapsens, I. Giovinazzo, J. Witte, C. Mondelli, S. Papadokonstantakis, K. Hungerbuehler and J. Pérez-Ramírez, *Energy Environ. Sci.*, 2015, **8**, 558.
- [3] Ecoinvent Centre, www.ecoinvent.org, accessed on 27/08/2015.
- [4] Available at www.pall.com/pdfs/Fuels-and.../FCBIODEN.pdf, retrieved on 27/08/2015
- [5] C. Rerat, S. Papadokonstantakis and K. Hungerbühler, *J. Air Waste Manage. Assoc.*, 2013, 349.
- [6] Available at www.ec.europa.eu/health/scientific_committees/consumer_safety/docs/scs_048.pdf, retrieved on 27/08/2015.
- [7] Available at http://www.sciencelab.com/msds.php?msdsId=9924778, retrieved on 27/08/2015.
- [8] Available at https://www.sciencelab.com/msds.php?msdsId=9922769, retrieved on 27/08/2015
- [9] A. Bridgwater, R. Chinthappali and P. Smith, *Identification and market analysis of most promising added-value products to be co-produced with the fuels*, Aston University, 2010.